European Review for Medical and Pharmacological Sciences 2024; 28: 4313-4325

Discovery of potential inhibitors targeting SARS-CoV-2 Mpro

W.-W. ZHOU[1], D.-S. LI[1], Y. CHEN[2], B.-Q. YOU[1], Y.-F. ZHENG[1], Y. LI[1], S.-Y. SI[1], J. ZHANG[1]

[1]Institute of Medicinal Biotechnology, Chinese Academy of Medical Sciences and Peking Union Medical College, Beijing, China
[2]Institute of Materia Medica, Chinese Academy of Medical Sciences and Peking Union Medical College, Beijing, China

W.-W. Zhou and D.-S. Li contributed equally to this work

Abstract. – OBJECTIVE: The coronavirus disease (COVID-19) pandemic, resulting from human-to-human transmission of a novel severe acute respiratory syndrome coronavirus (SARS-CoV-2), has caused a global health emergency. The lack of a specific drug or treatment strategy against this disease makes it devastating. Given that the main protease (Mpro) of SARS-CoV-2 plays an indispensable role in viral polyprotein processing, its successful inhibition prevents viral replication and constrains virus spread. Therefore, developing an effective SARS-CoV-2 Mpro inhibitor to treat COVID-19 is imperative.

MATERIALS AND METHODS: We employed a high-throughput screening (HTS) method based on fluorescence polarization (FP) assay and further confirmed by the fluorescence resonance energy transfer (FRET) method for the discovery of Mpro inhibitors. Then multiple approaches were taken to investigate the inhibition profiles of the hit compounds against Mpro, including 3-(4,5-dimethylthiazol-2-yl)-2,5-diphenyltetrazolium bromide (MTT) proliferation assay, surface plasmon resonance analysis (SPR), high-performance liquid chromatography-quadrupole-time-of-flight

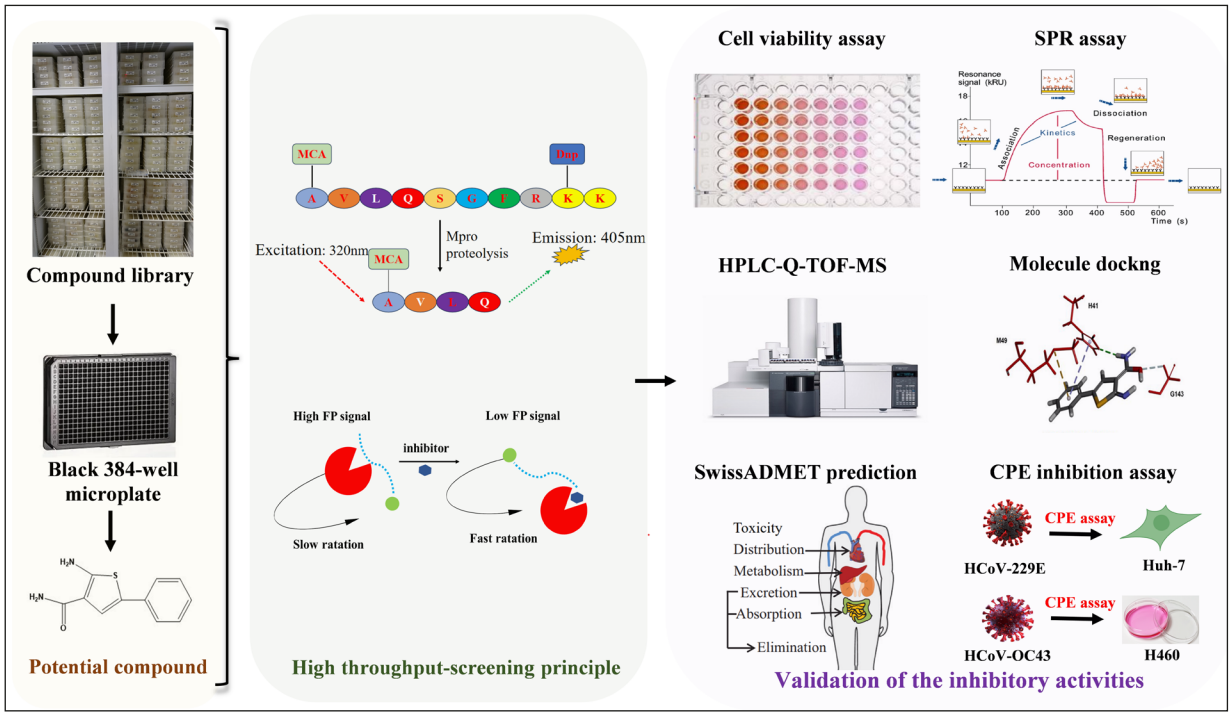

Graphical Abstract. High throughput screening and validation of inhibitors targeting SARS-CoV-2 Mpro.

Corresponding Authors: Yan Li, Ph.D; e-mail: liyan@imb.pumc.edu.cn;
Shuyi Si, Ph.D; e-mail: sisy@imb.pumc.edu.cn;
Jing Zhang, Ph.D; e-mail: jingjingz@imb.pumc.edu.cn

mass spectrometry (HPLC-Q-TOF-MS), cytopathic effect (CPE) assay, molecule docking, and the drug-likeness analysis.

RESULTS: **In this study, four Mpro inhibitors with low toxicity were selected from HTS. According to SPR, all the hit compounds had medium binding affinities toward SARS-CoV-2 Mpro. HPLC-Q-TOF-MS results revealed the non-covalent linkage of each compound with SARS-CoV-2 Mpro. Molecule docking simulated the molecule interactions between each compound and the substrate binding pocket of SARS-CoV-2 Mpro. CPE assay was used to detect their inhibitory activities against coronaviruses HCoV-OC43 and HCoV-229E. In particular, the IMB63-8G compound demonstrated the highest antiviral potency [50% effective concentration (IC_{50}) value of 1.71 μg/mL] and selectivity against HCoV-OC43 (SI = 39), which was more than 4-fold higher than that of ribavirin (RBV). Besides, the IMB63-8G compound possessed favorable drug-likeness characteristics.**

CONCLUSIONS: **Our results will highlight the therapeutic potential of these compounds for the treatment of SARS-CoV-2 infection.**

Key Words:
SARS-CoV-2, Mpro, HTS, Small molecule inhibitors.

Introduction

In late December 2019, the newly emerged highly contagious novel coronavirus disease 2019 (COVID-19) was identified in humans[1]. The outbreak of the virus containing a single positive-stranded RNA was first identified in Wuhan, China, and was named severe acute respiratory syndrome (SARS-CoV-2)[2]. The massive vaccination campaign for COVID-19 around the world was expected to result in herd immunity. These vaccines target the spike protein of the SARS-CoV-2 virus[3]. However, the spike protein is highly mutable, as confirmed by the new SARS-CoV-2 variants. Although booster vaccines may be developed for new variants, small molecule antivirals that have easier administration, delivery, storage, and production against less mutable targets will be more successful than a vaccine for COVID-19.

The search for new small molecules as drugs for COVID-19 includes proteolytic targets in SARS-CoV-2 infection: two viral proteases called main protease (Mpro) and papain-like protease (PLpro); three human proteases known as transmembrane protease serine 2 (TMPRSS2), cathepsin L and furin, angiotensin-converting enzyme 2 (ACE2), which is the receptor for spike, and an RNA-dependent RNA polymerase (RdRp) that is responsible for replicating the RNA genome[4]. Among these targets, the coronavirus Mpro has received significant attention due to its key role in enzymatic activity, leading to its posttranslational processing of replicase polyproteins[5,6]. During the replication cycle, the coronaviruses (CoVs) express two overlapping polyproteins (pp1a and pp1b) and four structural proteins from the viral RNA. Further proteolytic cleavage of these two viral polyproteins resulted in 16 non-structural proteins (nsp1–16). The PLpro manages the proteolytic cleaving of nsp1–3, whereas all junctions downstream of nsp4 are cleaved by Mpro, releasing the conserved key replicative functions, such as RNA-dependent RNA polymerase (RdRp), helicase, and three of the RNA processing domains[7]. In addition, unlike spike, the Mpro is a conserved protein across all coronaviruses[8]. The superposition of 12 crystal structures of Mpros (SARS-CoV-2, SARS-CoV, MERS-CoV, HCoV-HKU1, BtCoV-HKU4, MHV-A59, PEDV, FIPV, TGEV, HCoV-NL63, HCoV-229E, and IBV) revealed that all CoV Mpros share the same substrate-binding region between domains as a result of structure conservation[9]. Moreover, there are no human Mpro homologs, and it shares no overlapping substrate specificity with any known human protease, minimizing the possibility of side effects[10]. All these make it likely that inhibitors will have broad efficacy in potential future pandemics.

In the field of drug discovery, small molecule compounds are used to treat a variety of diseases and infections. The present work was undertaken to identify new potential inhibitors in the micromolar range against SARS-CoV-2 Mpro from the trove of small molecule compound library using miniaturized sandwich-like fluorescence polarization (FP)-based high-throughput screening (HTS) method. Subject to the extent of SARS-CoV-2 Mpro inhibition, the half-maximal inhibitory concentrations (IC_{50}) of the compounds of interest were determined using both FP and fluorescence resonance energy transfer (FRET) assay. Afterward, the selected compounds were evaluated using surface plasmon resonance (SPR), high-performance liquid chromatography-quadrupole-time-of-flight mass spectrometry (HPLC-Q-TOF-MS), and computational molecule docking calculations to ascertain their potential usefulness against SARS-CoV-2 Mpro. Each compound exhibited

molecule contacts with essential residues in the active pocket of SARS-CoV-2 Mpro in a non-covalent manner and medium affinity. Among the compounds screened, the IMB63-8G compound was found to have anti-HCoV-OC43 activity with no toxicity. The collected data related to IMB63-8G's drug-likeness potential using SwissADME studies[11] demonstrated that it had very high drug-likeness parameters with almost no metabolic disturbances. In this regard, the IMB63-8G compound may be the optimal potential candidate for use as an antiviral therapy in humans.

Materials and Methods

Chemicals, Regents, and Cell Lines

The compound libraries identified in this study were acquired from the National Center for Microbial Drug Screening, Institute of Medicinal Biotechnology (IMB), Chinese Academy of Medical Sciences (CAMS) and Peking Union Medical College (PUMC) (Beijing, China), which possessed ≥ 95% purity, were dissolved in Dimethyl sulfoxide (DMSO) at a final concentration of 10 mM and stored at -20°C before use.

The FRET fluorogenic substrate methoxycoumarine acetic acid (MCA)-Ala-Val-Leu-Gln-Ser-Gly-Phe-Arg-Lys(Dnp)-Lys-NH2 [(MCA-AVLQSGFRLys (Dnp)-Lys-NH2)] was purchased from Beyotime (Shanghai, China). FP tracer FITC-AVLQSGFRKK-Biotin [fluorescein isothiocyanate (FITC)-Ala (A)-Val (V)-Leu (L)-Gln (Q)-Ser-Gly-Phe-Arg-Lys-Lys-Biotin] was chemically synthesized by GenScript (Nanjing, China).

Huh-7 and H460 cell lines were cultured in Dulbecco's Modified Eagle's Medium (DMEM) supplemented with 10% fetal bovine serum (FBS). Cells were kept in a 37°C incubator and 5% CO_2 atmosphere. HCoV-229E and HCoV-OC43 were maintained in Yuhuan Li's lab (Key Laboratory of Antiviral Drug Research, IMB, CAMS and PUMC, Beijing, China). Mpro protein was provided by Yunyu Chen (Institute for Drug Screening and Evaluation, Wannan Medical College, Wuhu, Anhui, China).

FP-Based High-Throughput Primary Screening

The compounds used for HTS are from the synthetic and natural libraries of IMB and CAMS (Beijing, China). Stock compounds were maintained at the concentration of 10 mg/mL in 100% DMSO. FP screening assay was adopted for HTS primary screening according to a previous study. In total, 29 μL of Mpro (400 nM) diluted in the mP assay buffer was mixed with one μL of compound (1 mg/mL in DMSO) in a black 96-well microplate. Then, the mixture was incubated for 35 min at room temperature (RT) before adding the 20 μL of mP tracer (60 nM). After proceeding for 20 min at RT, the reaction was quenched by the addition of 10 μL of avidin (300 nM). The mP values were measured using a microplate reader. In each assay plate, GC-376 and DMSO were used as positive and negative controls, respectively. The well containing 60 μL of FITC-AVLQ peptide (20 nM) was used to assess the background noise. The inhibitory activity of the screening compound was calculated using the equation presented below. The compounds showing > 50% inhibition were considered as hit compounds in the primary screening.

$$\text{Inhibition (\%)} = \frac{Negative - Sample}{Negative - Positive} \times 100\%$$

The Inhibitory Activities of the Hit Compounds by FP

The dose-response relationship between the hit compounds' effect concentrations (1.56, 3.125, 6.25, 12.5, 25, 50, 100, and 200 μM) and Mpro activity regulation rate was determined according to the above method. The IC_{50} values of the compounds were calculated using GraphPad Prism 8 (San Diego, CA, USA).

Validation of the Inhibitory Activities of the Hit Compounds by FRET

The FRET assay described previously was adopted to further validate the inhibitory activities of the compounds[12]. Briefly, compounds (stock of 10 mM in 100% v/v DMSO) at various concentrations from 1.56 to 200 μM were pre-incubated with Mpro for 30 min at RT in black 96-well assay microplates (Corning, #3820, Corning, NY, USA). The fluorogenic substrate MCA-AVLQSGFR-Lys (Dnp)-Lys-NH2 was directly added to the enzyme/compound mix. After 5 min of incubation at RT, generation of the MCA-cleavage product/fluorescence signals was monitored at Ex/Em = 320/405 nm by EnVision (PerkinElmer, MA, USA). The reaction mixture contained 0.4 μmol/L purified enzyme, 5 μmol/L FRET substrate, 10 mM HEPES, 50 mM NaCl, 1 mM EDTA, and 1 mM DTT at a pH of 7.0. The results were fitted to

a normalized dose-response (variable slope) model in GraphPad 8 for IC_{50} characterization.

Cell Viability Assay

Cell viability was measured using the Cell Counting Kit-8 (CCK-8) (Promega Corporation, Fitchburg, Wisconsin, USA). Huh-7 and H460 cells were seeded at 5×10^3 cells/well in 96-well plates and incubated overnight before treatment. Compounds solubilized in DMSO were added to cells in an eight-point, two-fold serial dilution. The organic solvent in DMEM was < 0.1%. After 48 h, the contents of the wells were replaced with fresh medium containing 10% CCK-8 solution and were incubated at 37°C for 3 h. The final optical density at Optical $density_{450}$ (OD_{450}) was measured using an Envision 2104 multilabel reader (PerkinElmer Life Sciences, Waltham, MA, USA). The percentage of viable cells was calculated relative to cells treated with the solvent alone. The TC_{50} values of the compounds were calculated using GraphPad Prism 8.

SPR Assay

The binding affinity of compounds to SARS-CoV-2 Mpro was determined using a real-time SPR spectroscopy instrument (Reichert 2SPR, Buffalo, NY, USA). The Mpro protein was immobilized onto a surface-activated CM5 gold biosensor (Reichert Inc., New York, NY, USA), and the active sites were quenched with 1 M ethanolamine buffer (pH of 8.0). The compounds were injected as analytes at various concentrations with a contact time of 90 s, and the dissociation kinetic was recorded at 330 s. The real refractive index unit (RIU) was continuously monitored and is related to the arbitrary resonance unit (RU) as 1 μRIU = 0.733 RU. Both association (K_{on}) and dissociation (K_{off}) constant values were determined with TraceDrawer 1.7.1 (Ridgeview Instruments, Uppsala, Sweden). $K_d = K_{off}/K_{on}$

Intact Protein Analysis

Purified SARS-CoV-2 Mpro (5 μM) was incubated in the presence or absence of compounds (500 μM) in tris buffered saline (TBS) (10 mM Tris and 50 mM NaCl at pH of 8.0) at RT for 30 min. The molecule weight of the free SARS-CoV-2 Mpro and compound-treated SARS-CoV-2 Mpro were detected by the quadrupole time-of-flight (Q-TOF) mass spectrum (Agilent, Santa Clara, CA, USA). The mass spectrum was deconvoluted using MassHunter software (Agilent, Santa Clara, CA, USA), and maximum entropy was performed for the deconvoluting algorithm. Mass spectrum data were saved and processed using FlexControl 3.4 (FLEXCONTROL, Noerre Nebel, Denmark).

Molecule Docking

The structure of SARS-CoV-2 Mpro was retrieved from the co-crystal structure on the Protein Data Bank (PDB) (PDB code: 7D3I)[13]. The molecule simulation docking of the compounds into the binding site of SARS-CoV-2 Mpro was explored using the BIOVIA Discovery Studio 2018R2 software (BIOVIA, Dassault Systemes, Paris, France). The water molecules and cofactors were removed from the protein, and the possible binding pocket in Mpro was defined according to previous publications[13,14]. After identifying the potential hydrogen-bond interactions between the catalytic sites of Mpro and the compounds, the C-DOCKER program (BIOVIA, Dassault Systemes, Paris, France) was used to generate and process the optimized docking result.

Cytopathic Effect (CPE) Inhibition Assay

The anti-coronavirus activity of the four compounds was determined using a CPE inhibition assay. Briefly, cells were plated into 96-well culture plates and incubated for 24 h. The cells were infected with 10^{-3} HCoV-229E or HCoV-OC43 and the indicated concentrations of compounds were added simultaneously. HCoV-229E-infected Huh7 cells and HCoV-OC43-infected H460 cells were treated in an atmosphere of 5% CO_2 and 35°C until the CPE of the virus control group reached 4+. The half maximal inhibitory concentration (IC_{50}) was determined using the Reed-Muench method[15]. The selectivity index (SI) was calculated as the ratio of the 50% toxic concentration (TC_{50})/IC_{50}.

SwissADMET Prediction for the Compounds

The SwissADME server (available at: http://www.swissadme.ch/) is a network tool that provides the prediction of pharmaceutically significant descriptors and physically relevant properties of the compounds, including the physicochemical properties (molar refractivity, topological polar surface area, and a number of hydrogen bond donors/number of hydrogen bond acceptors), lipophilicity (logPO/w), pharmacokinetics properties [gastrointestinal absorption, blood-brain barrier permeability, P-gp substrate, cytochrome-P en-

zyme inhibition, and skin permeation (log Kp)], which are critical parameters for the prediction of drug absorption and distribution in the body. Additionally, drug-likeness (Lipinski's rule of five) was predicted using SwissADME[11]. The structures of the hit compounds were converted into the SMILES format using ChemDraw software (CambridgeSoft, Cambridge, MA, USA). Then, the "run to" operation was used to predict the pharmacokinetics of the compounds.

Statistical Analysis

The *t*-test was used to determine the difference between treatment groups and the control. All data are expressed as mean ± standard deviation (SD) and were analyzed using GraphPad Prism 8 (GraphPad Software, Boston, MA, USA).

Results

Screening for Candidates of SARS-CoV-2 Mpro Inhibitors

(i) Primary HTS of hit compounds against SARS-CoV-2 Mpro activity

An HTS platform was previously established using FP-based peptide substrates to discover novel small molecule weight inhibitors against SARS-CoV-2 Mpro[16]. A fluorescein isothiocyanate (FITC) and biotin dual-labeled small peptide FITC-AVLQSGFRKK-Biotin (FITC-S-Biotin), which was generated from previously used FRET substrate, was used as the FP tracer. This FP tracer can be hydrolyzed by active Mpro to yield two peptide fragments, FITC-AVLQ and SGFRKK-Biotin, yielding a low FP signal. In the presence of Mpro inhibitors, the uncleaved FP tracer will bind to the large binding partner avidin and result in a high mP value. Using this screening assay, dieckol, a natural phlorotannin component extracted from a Chinese traditional medicine *Ecklonia cava*, was identified as a novel competitive inhibitor against SARS-CoV-2 Mpro *in vitro*[16], proving its feasibility.

In this research, over 50,000 compounds were tested for SARS-CoV-2 Mpro inhibitory activity at 33 μg/mL. Compounds with inhibition rates higher than 50% were selected for follow-up in-depth research. Four compounds, namely IMB63-8G, IMB84-8D, IMB26-11E, and IMB96-2A, maintained stable inhibitory activities above 50%. Their structures are shown in Figure 1A.

(ii) Inhibitory effects of the hit compounds on SARS-CoV-2 Mpro

To further evaluate the inhibitory activities of the four compounds against SARS-CoV-2 Mpro, IC_{50} values of IMB63-8G, IMB84-8D, IMB26-11E, and IMB96-2A were detected with an FP assay. The results are shown in Figure 1A, which were 14.75 ± 8.74, 67.69 ± 10.18, 41.53 ± 4.01, and 44.43 ± 8.07 μM, respectively. GC-376, an oral-specific drug targeting SARS-CoV-2 Mpro, was used as a positive control, with an IC_{50} of 5.13 ± 0.41 μM (Figure 1B).

FRET assay, a classic method to detect the inhibitory activity of Mpro inhibitors, was used to confirm the inhibitory activity of the four compounds on the Mpro[17]. Similar results were obtained: The ICs_{50} of IMB63-8G, IMB84-8D, IMB26-11E, and IMB96-2A compounds were 16.27 ± 0.62, 24.25 ± 3.35, 32.48 ± 5.19, and 38.36 ± 6.16 μM, respectively (Figure 1C). GC-376 showed an IC_{50} value of 4.20 ± 2.06 μM with this method, consistent with the reported value (Figure 1C)[18].

Detection for Binding Mode of the Four Hit Compounds with SARS-CoV-2 Mpro

(i) Affinity of the four compounds for SARS-CoV-2 Mpro

SPR biosensor-based assay was performed to elucidate the binding mechanisms of the four compounds with SARS-CoV-2 Mpro. SPR is an optical biosensor detection method that measures the interaction between ligand and analyte by monitoring the change in the refractive index of the surface interface that occurs during the binding process.

The Mpro protein was immobilized on a Carboxymethyl Dextran sensor chip, and then the compound flowed through the chip. As shown in Figure 2A, all four compounds could bind with Mpro in a concentration-dependent manner. The result also indicated a simulated interaction mode of all the hit compounds, with Mpro showing a steady state upon injection after rapid combination, as well as rapid dissociation from the binding site for compounds IMB63-8G and IMB26-11E and slow dissociation for compounds IMB84-8D and IMB96-2A. The K_d value reflects the affinity of the compound for the target, with smaller values indicating stronger affinity. Table I and Figure 2A indicate that all four compounds showed comparable moderate binding ability with Mpro (1.06×10^{-4} M for

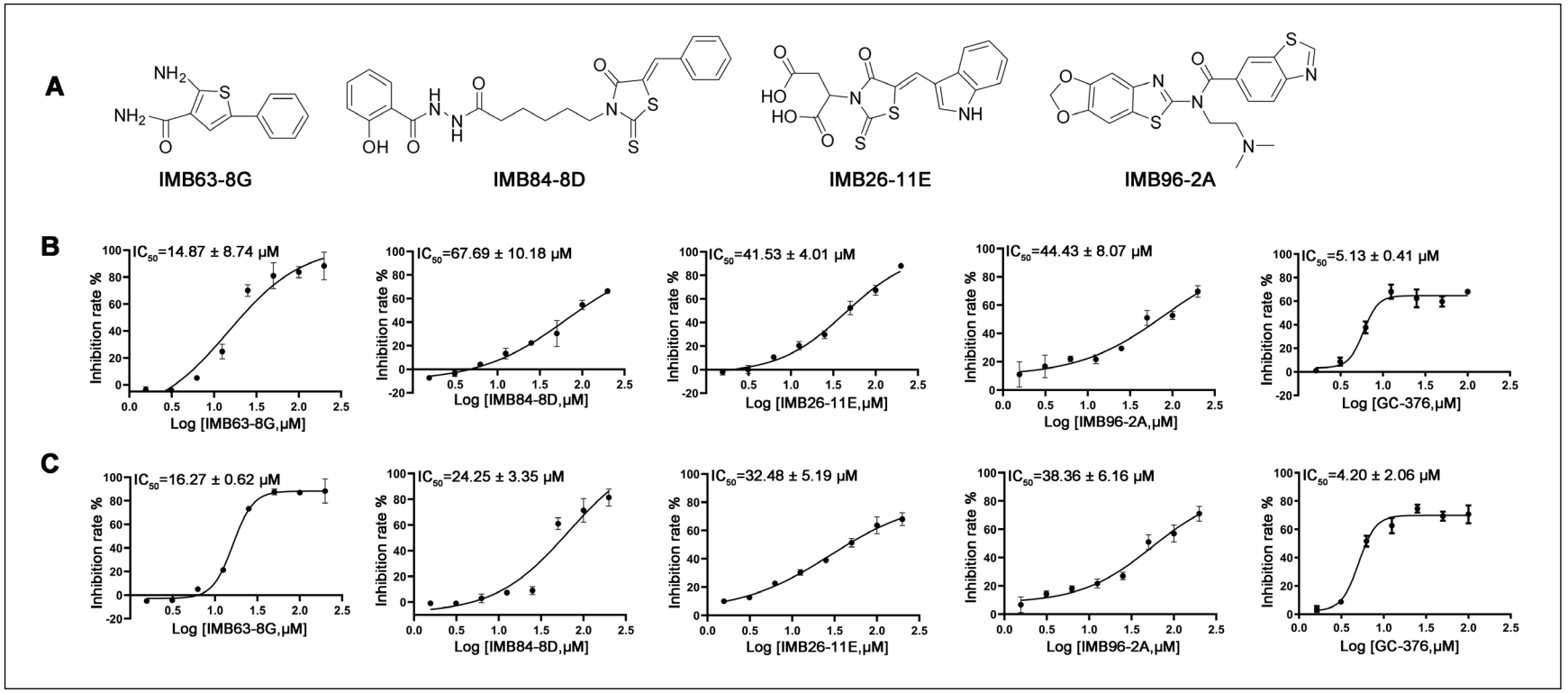

Figure 1. Inhibitory activity profiles of the hit compounds against SARS-CoV-2 Mpro. **A**, Structures of the hit compounds. **B**, FP-based enzymatic assay. Different concentrations of compounds (from 1.56 μM to 200 μM) were added to the FP reaction system, and changes in the relative cleaving activity of SARS-CoV-2 Mpro with FITC-AVLQSGFRKK-Biotin [fluorescein isothiocyanate (FITC)-Ala (A)-Val (V)-Leu (L)-Gln (Q)-Ser-Gly-Phe-Arg-Lys-Lys-Biotin] as the substrate were detected. **C**, Fluorescence resonance energy transfer (FRET)-based enzymatic assay. Compounds at various concentrations from 1.56 μM to 200 μM were pre-incubated with Mpro for 30 min at RT, and then the fluorogenic substrate methoxycoumarine acetic acid (MCA)-Ala-Val-Leu-Gln-Ser-Gly-Phe-Arg-Lys(Dnp)-Lys-NH2 [(MCA-AVLQSGFRLys (Dnp)-Lys-NH2)] was added. Generation of the MCA-cleavage product/fluorescence signals was monitored (Ex/Em = 320/405 nm). GC-376 was used as a positive control. Data are shown as mean ± SD, n = 3.

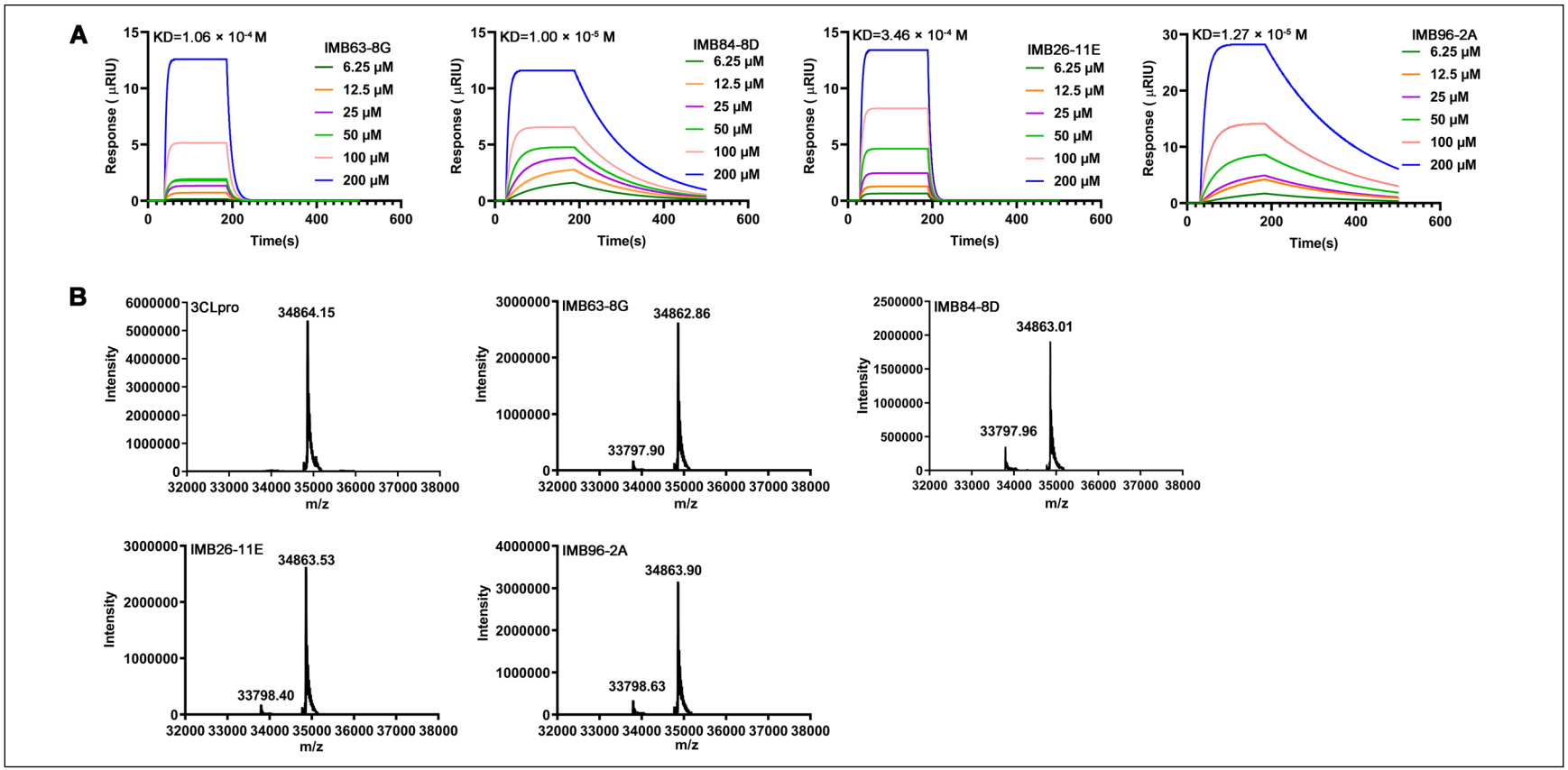

Figure 2. Detection for the binding mode of the hit compounds with SARS-CoV-2 Mpro. **A**, SPR analysis of the interaction between each hit compound with SARS-CoV-2 Mpro. Mpro protein was immobilized on the CM5 sensor chip, and then the compound at various concentrations (from 6.25 μM to 200 μM) flowed through the chip. The kinetics of the compound were evaluated according to the change in the RIU value. The change in response units was shown. **B**, The hit compounds interacted non-covalently with SARS-CoV-2 Mpro. Purified SARS-CoV-2 Mpro (5 μM) was incubated in the presence or absence of compounds (500 μM) in tris buffered saline (TBS) at room temperature (RT) for 30 min. The molecular weights of SARS-CoV-2 Mpro with each hit compound were determined using high-performance liquid chromatography-quadrupole-time-of-flight mass spectrometry (HPLC-Q-TOF-MS). The mass shift (Δm) of the protein is labeled.

Table I. The kinetics evaluation of the SPR interactions.

Compounds	K_{on} (1/M*S)	K_{off} (1/S)	$K_d = K_{off}/K_{on}$ (M)
IMB63-8G	8.78×10^{2}	9.28×10^{-2}	1.06×10^{-4}
IMB84-8D	7.88×10^{2}	7.88×10^{-3}	1.00×10^{-5}
IMB26-11E	4.33×10^{2}	1.50×10^{-1}	3.46×10^{-4}
IMB96-2A	3.83×10^{2}	4.85×10^{-3}	1.27×10^{-5}

K_{on}: association rate constant; K_{off}: dissociation rate constant; K_d (dissociation constant) = K_{off}/K_{on}.

IMB63-8G, 1.00 × 10^{-5} M for IMB84-8D, 3.46 × 10^{-4} M for IMB26-11E, and 1.27 × 10^{-5} M for IMB96-2A).

(ii) HPLC-Q-TOF-MS Based Study of SARS-CoV-2 Mpro Association with the Hit Compounds

To obtain insight into the hit compounds' binding mode to SARS-CoV-2 Mpro, we performed HPLC-Q-TOF-MS to determine the change in molecule weights in the presence and absence of the compounds. After preincubation with each compound respectively, the molecule weights remained the same when compared to Mpro alone (34,862.86 Da) (Figure 2B), reflecting non-covalent binding.

Docking of the Hit Compounds to SARS-CoV-2 Mpro Structure

To further evaluate the possible binding sites of compounds and enzymes, an *in silico* docking simulation was performed to predict the amino acid residues in SARS-CoV-2 Mpro that interacted with the four compounds. The reported crystal structure of SARS-CoV-2 Mpro in complex with MI-23 (PDB code: 7D3I) was retrieved as the docking target. As shown in Figure 3, these four compounds fit within the substrate binding pocket of SARS-CoV-2 Mpro with slightly different binding modes. IMB63-8G compound formed a hydrogen bond (2.53 Å) and a pi–pi interaction (5.31 Å) with His41, whereas it formed a pi–sulfur interaction (4.44 Å) with Met49 and

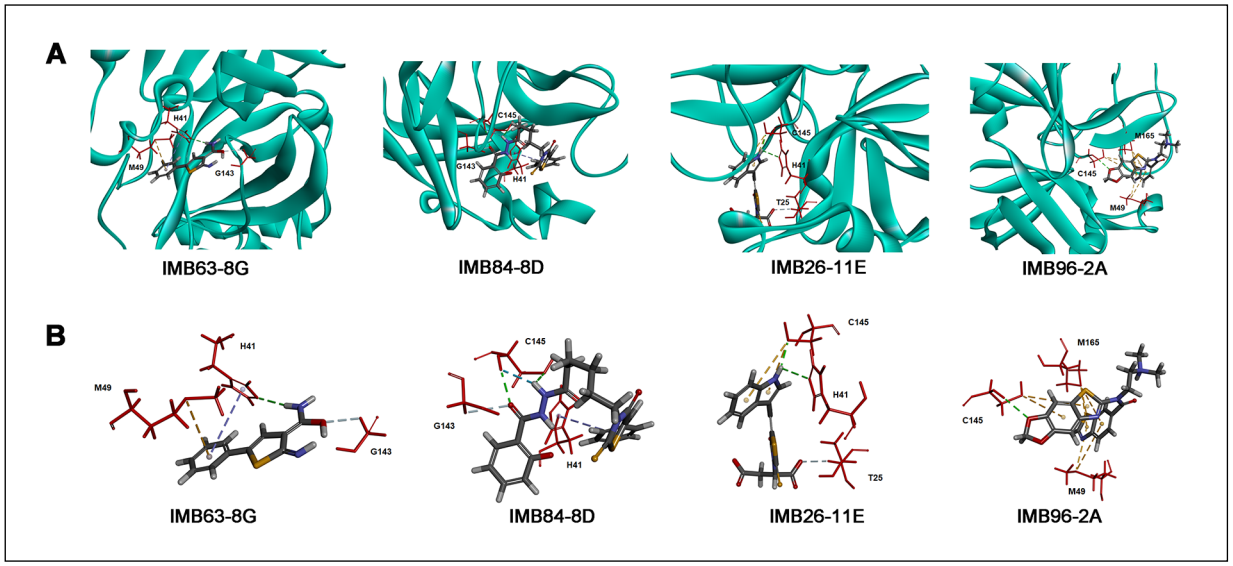

Figure 3. Docking poses of the hit compounds with the active site of SARS-CoV-2 Mpro (PDB code: 7D3I). **A**, Molecular modeling of the hit compounds in the binding pocket of SARS-CoV-2 Mpro. The red sticks represent the functional amino acids interacting with the hit compounds, which are exhibited by a stick model. **B**, Detailed illustration for each hit compound binding to the catalytic residues of SARS-CoV-2 Mpro. Strong hydrogen-bond interactions are highlighted by the green dashed lines. The purple dashed line indicates pi–pi interaction. Yellow dashes represent pi–sulfur interaction. Blue dashes depict the unfavorable donor–donor interaction. Carbon-hydrogen bond interaction is shown as gray dashed lines. Pink dashes indicate pi-alkyl interaction.

a carbon-hydrogen bond with Gly143 (2.98 Å). As for the binding of IMB84-8D, hydrogen bonds (2.35 Å and 2.35 Å) and an unfavorable donor–donor interaction (2.47 Å) were observed at the catalytic residue Cys145, whereas a pi–pi interaction (4.71 Å) with His41 and a carbon-hydrogen bond was observed with Gly143 (2.96 Å). When the IMB26-11E compound was docked to Mpro, it formed a hydrogen bond (2.08 Å) and two pi–sulfur interactions (5.33 Å and 4.12 Å) with Cys145, whereas it formed a hydrogen bond (2.73 Å) with His41 and a carbon-hydrogen bond (2.49 Å) with Thr25. In terms of IMB96-2A compound, it interacted with Cys145 through a hydrogen bond (2.67 Å) and a pi–sulfur interaction (4.43 Å), whereas it interacted with Met165 through three pi–sulfur interactions (4.49 Å, 3.09 Å, and 5.59 Å) and Met49 through sulfur interactions (5.13 Å and 4.26 Å).

In conclusion, all four compounds could occupy the active site and interact with either of the two key catalytic residues of Mpro His41 and Cys145 (compounds IMB63-8G and 96-2A) or both of them (compounds IMB84-8D and 26-11E)[19]. Since the presence of hydrogen bonds contributes more to the binding affinity of the Mpro inhibitor, all compounds interact with Mpro through one or two hydrogen bonds.

Antiviral Activities of the Hit Compounds Against HCoV-229E and HCoV-OC43

CPE assay was used to detect the inhibitory activities of the four compounds against coronaviruses HCoV-229E and HCoV-OC43, as well as their toxicity in the corresponding cells. Ribavirin (RBV) was used as a positive control. As shown in Table II, only the IMB63-8G compound and RBV can inhibit the CPE induced by HCoV-OC43 infection in H460 cells. TC_{50} of IMB63-8G was 66.67 μg/mL, the IC_{50} against HCoV-OC43 was 1.71 μg/mL, and SI was 39, which were much higher than those of RBV (Table II). With regard to HCoV-229E, none of the compounds could inhibit the CPE induced by HCoV-229E infection in Huh-7 cells.

Drug Ability Evaluation of IMB63-8G

Drug discovery and development depend heavily on assessing absorption, distribution, metabolism, and excretion (ADME) characteristics. The pharmacokinetics and drug-likeness prediction of IMB63-8G was performed using the online tool SwissADME (available at: http://www.swissadme.ch/index.php)[20].

Drug-likeness analysis of the bioactive IMB63-8G with different parameters is tabulated (Table III) and shown in a SwissADME bioavailability radar (Figure 4A) and diagram of the molecular formula BOILED egg (Figure 4B). IMB63-8G showed good binding affinity against SARS-CoV-2 Mpro with high drug-likeness parameters, good solubility with log S not higher than 6[11] and high GI absorption (Table III). It also predicted a high probability of passive absorption by the gastrointestinal tract (white region) but not accessing the brain penetrant (yellow region) (Figure 4B). As a transmembrane protein, permeability glycoprotein (P-gp) could actively transport a wide variety of chemically diverse compounds out of the cell[21]. If the compound is the substrate of P-gp, it may be excreted from the cell, and thus affect the therapeutic effect. IMB63-8G is forecasted to be non-substrate of P-gp. Additionally, it is the only inhibitor of two CYP enzymes (CYP1A2 and CYP 2C19) and is specific in nature [zero alert for PAINS (pan assay interference compounds)].

Discussion

SARS-CoV-2 was recognized as the cause of the atypical pneumonia outbreak in Wuhan, China. It has now almost paralyzed the globe and has not only distressed the health and welfare of humans

Table II. Anti-HCoV-OC43 activities of the compounds in H460 cells.

Compounds	TC_{50} (μg/mL)	IC_{50} (μg/mL)	SI
IMB63-8G	66.67	1.71	39.0
IMB84-8D	12.83	> 7.41	-
IMB26-11E	> 200	> 200	-
IMB96-2A	> 200	> 66.67	-
RBV	77.61	8.62	9.0

RBV: ribavirin; TC_{50}: half maximal toxic concentration; IC_{50}: half maximal inhibitory concentration; SI: selectivity index = TC_{50}/IC_{50}.

Table III. Drug-likeness of IMB63-8G.

HB donors[a]	HB acceptors[a]	No. of rotatable bond[a]	Consensus log P[a]	Log S (ESOL)[b]	Log S (Ali)[b]	Log S (SILICOS-IT)[b]	GI absorption[c]	CYP enzymes inhibitors[c]
2	1	2	1.98	-3.08	-4.02	-3.42	High	CYP1A2, CYP2C19 inhibitor

[a]: Physicochemical properties; [b]: solubility; [c]: pharmacokinetics; HB: hydrogen bonding; GI: gastrointestinal; CYP: cytochrome $P4_{50}$ proteins; ESOL: a method used to predict water solubility. It stands for estimating aqueous solubility directly from molecular structure followed by molecular weight, the proportion of heavy atoms in an aromatic system, and the number of rotatable bonds. SILICOS-IT: another method used to predict the water solubility. Log (SILICOS-IT) determines the negative logarithm of water solubility of a compound by fragmental method.

but also imposed burdens on worldwide economic activity and development. Current COVID-19 vaccines target the spike protein of SARS-CoV-2, the pathogen of COVID-19. Yet, the spike is a weakly conserved protein in a highly mutable RNA virus. Although SARS-CoV-2 shares an overall 82% genome sequence identity with SARS-CoV, the spike has only 76% protein sequence identity shared between two origins[22]. The highly mutable nature of the spike has also been corroborated by the continuous identification of new SARS-CoV-2 variants with spike mutations[23]. Accumulating evidence[24] has shown attenuated activity of the approved vaccines against certain new SARS-CoV-2 variants. Furthermore, the selective pressure from spike-specific antibodies induced from a vaccine or original SARS-CoV-2 infection could promote the acquisition of additional mutations to cause a change in viral antigenicity that would allow the SARS-CoV-2 variants to escape from immune responses[25]. The continuing threat to global health posed by the SARS-CoV-2 and its variants with increased abilities to spread and escape from immunity demands an arsenal of approaches and drug modalities that should likely include small molecules as antiviral agents that target proteins other than the spike protein to effectively combat the COVID-19 pandemic.

Targeting the components responsible for replication of SARS-CoV-2 is considered a good strategy to identify effective drugs for the treatment of COVID-19. The coronavirus Mpro is a cyste-

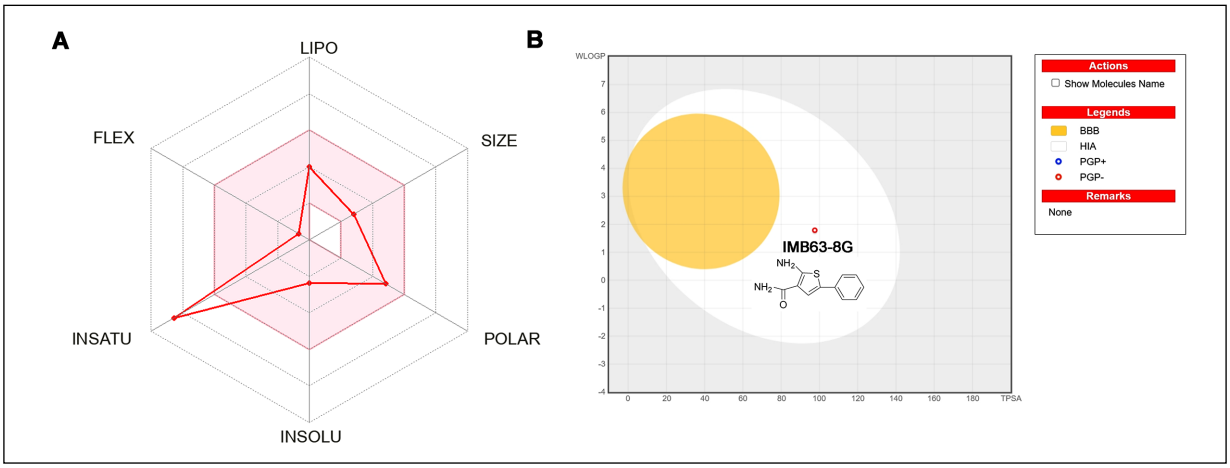

Figure 4. SwissADME analysis for IMB63-8G. **A**, Radar plot of the IMB63-8G compound after calculating ADME data. The pink area represents the optimal range for each property (clockwise from top, lipophilicity: XLOGP3 between -0.7 and +5.0, size: MW between 150 and 500 g/mol, polarity: TPSA between 20 and 130 Å2, solubility: log S ≤ 6, saturation: fraction of carbons in the sp3 hybridization ≥ 0.25, and flexibility: ≤ 9 rotatable bonds). **B**, Diagram of molecular formula BOILED egg for IMB63-8G. The white region stands for a high probability of passive absorption by the gastrointestinal tract, and the yellow region (yolk) stands for a high probability of brain penetration. Besides, the blue dot represents P-gp substrates (PGP+), and the red dot represents P-gp non-substrate (PGP-).

ine protease that cleaves the polyproteins at 11 positions and allows for the assembly of the viral replicase complex[26]. Unlike spike, Mpro is highly conserved. In total, 96% of its protein sequence identity is shared between SARS-CoV[3]. Given its crucial role in virus replication and distinguishing characteristics, the SARS-CoV-2 Mpro is a prominent drug target for COVID-19 antiviral therapy.

A number of small molecule inhibitors of SARS-CoV-2 Mpro have been reported[27-33] in the past three years. Most of these compounds were obtained by protein structure-based rational design and chemical synthesis. In this study, we focused on the discovery of small molecule compounds through FP-based SARS-CoV-2 Mpro enzymatic assay to explore a library of small molecule compounds. Among the 50,000 compounds screened, we found that four compounds exhibited SARS-CoV-2 Mpro inhibitory activities with low toxicity. The binding profiles of the four compounds revealed that they could form hydrogen bonds with multiple residues located at the active site of Mpro, where successful protease inhibition occludes the accessibility of the substrate binding site and the catalytic residues. Based on the HPLC-Q-TOF-MS analysis, the molecule weights of Mpro before and after its incubation with the compounds using HPLC-Q-TOF-MS remained unchanged, indicating non-covalent conjugation between the compounds with Mpro. Combined techniques of molecule docking and HPLC analysis suggested that the mechanisms may be related to non-covalent interactions. This mechanism is different from most previously reported[34] Mpro inhibitors, which could form covalent bonds with protein residues. Among them, the IMB63-8G compound could remarkably inhibit the HCoV-OC43 virus with IC_{50} of 1.71 μg/mL.

In this research, we combined FP and FRET assays to confirm the hit compounds' inhibitory activities. FP assay adopted a FITC and biotin dual-labeled small peptide as its tracer. The highly active Mpro can adequately hydrolyze this tracer to yield two peptide fragments, FITC-peptide fragment and peptide fragment-Biotin. This FITC-peptide fragment with smaller molecular weight could not bind to the large protein avidin due to the absence of Biotin and will result in a low FP signal. On the other hand, in the absence of Mpro, the intact FP tracer is bound to avidin, exhibiting a high FP signal. The principle of the FRET assay is as follows: the C-terminal of a peptide substrate links to a fluorophore, and the N-terminal has a fluorescence quencher that quenches the fluorescence signal of the fluorophore. When the Mpro hydrolyzes the substrate to yield two fragments, the fluorescence quencher is separated with a fluorophore, which relieves the fluorescence quenching effect, resulting in an increase of fluorescence signal[35]. Both of the assays have limitations. In a FRET screening assay, the fluorescence interferences from natural products indeed could quench the emission fluorescence of a FRET fluorogenic substrate (320/405 nm), and the false positives are inevitably present in the screen due to the presence of inherent fluorescence from the compounds being tested[36]. In contrast to our developed FP screening assay, the effect of potential fluorescent interferences is minimized because the used fluorophore, FITC, has a high quantum yield for emission at 535 nm wavelength, which is outside the range of many fluorescent molecules in natural product screening. However, the possible fluorescent interferences still exist in an FP screening assay. So, the inhibitory activities of the hit compounds were separately evaluated using both assays. It is worth mentioning that the inhibitory activity and SI of IMB63-8G are significantly higher than those of the positive control RBV. ADMET analysis implied that the IMB63-8G compound had all favorable parameters, including low but suitable aqueous solubility, favorable oral bioavailability values, and mild to low toxicity.

Conclusions

For the first time, we reported the anti-Mpro activities of four compounds from HTS based on a combination of FP and FRET assay. Among them, IMB63-8G may be the most suitable compound for further drug evaluation as an inhibitor of SARS-CoV-2 Mpro. However, additional studies, such as antiviral activities against SARS-CoV-2 and laboratory tests *in vivo* on animals, are necessary to approve its validity in inhibiting COVID-19.

Acknowledgments

We are grateful to senior engineer Zhensheng Xie (Institute of Biophysics, Chinese Academy of Sciences, Beijing, China) for her kind help in HPLC-QTOF-MS analysis, Yunyu Chen (Institute for Drug Screening and Evaluation, Wannan Medical College) for assistance with FP and FRET assay and providing the Mpro, and Yuhuan Li and Rongmei Gao (Key Laboratory of Antiviral Drug Research, Institute of Medicinal Biotechnology, Chinese Academy of Medical Sciences and Peking Union Medical College) for testing the cytopathic effects of the hit compounds infected by human coronavirus HCoV-229E and HCoV-OC43. Last, we would

like to thank LetPub (www.letpub.com) for its linguistic assistance during the preparation of this manuscript.

Funding

This work was supported by the CAMS Innovation Fund for Medical Sciences (CIFMS) (No. 2022-I2M-2-002, No. 2021-I2M-1-054) and the National Natural Science Foundation of China (No. 81370087).

Authors' Contributions

Wenwen Zhou and Dongsheng Li performed the experiments and wrote the manuscript. Ying Chen was involved in the virtual docking. Baoqing You conducted the ADMET analysis and the final editing of the manuscript. Yifan Zheng analyzed the data. Yan Li, Shuyi Si and Jing Zhang were responsible for the research design and the original draft polishing. All authors have read and agreed to the published version of the manuscript.

Conflicts of Interest

All authors declare no conflict of interest.

Data Availability

All data generated or analyzed during this study are included in this article or are available from the authors upon request.

Informed Consent

Not applicable due to the design of the study.

Ethics Approval

Ethical review and approval were waived due to the design of the study.

ORCID ID

Wen-Wen Zhou: 0009-0002-8113-2699
Dong-Sheng Li: 0000-0001-5348-4764
Bao-Qing You: 0009-0001-5977-2537
Yi-Fan Zheng: 0009-0000-5589-8186
Yan Li: 0009-0009-6675-8096
Shu-Yi Si: 0000-0003-4422-6848
Jing Zhang: 0000-0003-2299-1979

AI Disclosure

The authors did not use any AI tools for the preparation of the manuscript.

References

1) Zhu N, Zhang D, Wang W, Li X, Yang B, Song J, Zhao X, Huang, Shi WF, Lu R, Niu PH, Zhan FX, Ma XJ, Wang DY, Xu WB, Wu GZ, Gao GF, Tan WJ. A Novel Coronavirus from Patients with Pneumonia in China, 2019. N Engl J Med 2020; 382: 727-733.
2) Hu B, Guo H, Zhou P, Shi ZL. Characteristics of SARS-CoV-2 and COVID-19. Nat Rev Microbiol 2021; 19: 141-154.
3) Morse JS, Lalonde T, Xu S, Liu WR. Learning from the Past: Possible Urgent Prevention and Treatment Options for Severe Acute Respiratory Infections Caused by 2019-nCoV. Chembiochem 2020; 21: 730-738.
4) Joshi S, Joshi M, Degani MS. Tackling SARS-CoV-2: proposed targets and repurposed drugs. Future Med Chem 2020; 12: 1579-1601.
5) Peele KA, Potla Durthi C, Srihansa T, Krupanidhi S, Ayyagari VS, Babu DJ, Indira M, Reddy AR, Venkateswarulu TC. Molecular docking and dynamic simulations for antiviral compounds against SARS-CoV-2: A computational study. Inform Med Unlocked 2020; 19: 100345.
6) Das S, Sarmah S, Lyndem S, Singha Roy A. An investigation into the identification of potential inhibitors of SARS-CoV-2 main protease using molecular docking study. J Biomol Struct Dyn 2021; 39: 3347-3357.
7) Ullrich S, Nitsche C. SARS-CoV-2 Papain-Like Protease: Structure, Function and Inhibition. Chembiochem 2022, 23: e202200327.
8) Mengist HM, Dilnessa T, Jin T. Structural Basis of Potential Inhibitors Targeting SARS-CoV-2 Main Protease. Front Chem 2021; 9: 622898.
9) Jin Z, Du X, Xu Y, Deng Y, Liu M, Zhao Y, Zhang B, Li XF, Zhang LK, Peng C, Duan YK, Yu J, Wang L, Yang K, Liu FJ, Jiang RD, Yang XL, You T, Liu XC, Yang XN, Bai F, Liu H, Liu X, Guddat LW, Xu WQ, Xiao GF, Qin CF, Shi ZL, Jiang HL, Rao ZH, Yang HT. Structure of M(pro) from SARS-CoV-2 and discovery of its inhibitors. Nature 2020; 582: 289-293.
10) Kim Y, Liu H, Galasiti Kankanamalage AC, Weerasekara S, Hua DH, Groutas WC, Chang KO, Pedersen NC. Reversal of the Progression of Fatal Coronavirus Infection in Cats by a Broad-Spectrum Coronavirus Protease Inhibitor. PLoS Pathog 2016; 12: e1005531.
11) Daina A, Michielin O, Zoete V. SwissADME: a free web tool to evaluate pharmacokinetics, drug-likeness and medicinal chemistry friendliness of small molecules [J]. Sci Rep 2017; 7: 42717.
12) Ahuja R, Kaur A, Kumari G, Kumar A, Kumar S, Roy AK, Majumdar T. Enhanced expression and solubility of main protease (Mpro) of SARS-CoV-2 from E. coli, Protein Expr Purif 2021; 211: 106337.
13) Qiao J, Li YS, Zeng R, Liu FL, Luo RH, Huang C, Wang YF, Zhang J, Quan B, Shen C, Mao X, Liu X, Sun W, Yang W, Ni X, Wang K, Xu L, Duan ZL, Zou QC, Zhang HL, Qu W, Long YH, Li MH, Yang RC, Liu X, You J, Zhou Y, Yao R, Li WP, Liu JM, Chen P, Liu Y, Lin GF, Yang X, Zou J, Li L, Hu Y, Lu GW, Li WM, Wei YQ, Zheng YT, Lei J, Yang S. Yang, SARS-CoV-2 M(pro) inhibitors with antiviral activity in a transgenic mouse model. Science 2021; 371: 1374-1378.

14) Jin Z, Zhao Y, Sun Y, Zhang B, Wang H, Wu Y, Zhu Y, Zhu C, Hu T, Du X, Duan Y, Yu J, Yang X, Yang X, Yang K, Liu X, Guddat LW, Xiao G, Zhang L, Yang H, Rao Z. Structural basis for the inhibition of SARS-CoV-2 main protease by antineoplastic drug carmofur. Nat Struct Mol Biol 2021; 27: 529-532.

15) Li Z, He Y, Ge L, Quan R, Chen J, Hu Y, Sa R, Liu J, Ran D, Fu Q, Shi H. Berbamine, a bioactive alkaloid, suppresses equine herpesvirus type 1 in vitro and in vivo. Front Vet Sci 2023; 10: 1163780.

16) Yan G, Li D, Lin Y, Fu Z, Qi H, Liu X, Zhang J, Si S, Chen Y. Development of a simple and miniaturized sandwich-like fluorescence polarization assay for rapid screening of SARS-CoV-2 main protease inhibitors [J]. Cell Biosci 2021; 11: 199.

17) Ihssen J, Faccio G, Yao C, Sirec T, Spitz U. Fluorogenic in vitro activity assay for the main protease M(pro) from SARS-CoV-2 and its adaptation to the identification of inhibitors. STAR Protoc 2021; 2: 100793.

18) Fu L, Ye F, Feng Y, Yu F, Wang Q, Wu Y, Zhao C, Sun H, Huang B, Niu P, Song H, Shi Y, Li X, Tan W, Qi J, Gao GF. Both Boceprevir and GC376 efficaciously inhibit SARS-CoV-2 by targeting its main protease. Nat Commun 2020; 11: 4417.

19) Zhao Y, Sun Y, Zhang B, Wang H, Wu Y, Zhu Y, Zhu C, Hu TY, Du XY, Duan YK, Yu J, Yang XB, Yang XN, Yang KL, Liu X, Guddat LW, Xiao GF, Zhang LK, Yang HT, Rao ZH. Structural basis for the inhibition of SARS-CoV-2 main protease by antineoplastic drug carmofur. Nat Struct Mol Biol 2020; 27: 529-532.

20) Zoete V, Daina A, Bovigny C, Michielin O. SwissSimilarity: A Web Tool for Low to Ultra High Throughput Ligand-Based Virtual Screening. J Chem Inf Model 2016; 56: 1399-1404.

21) Mora Lagares L, Minovski N, Novič M. Multiclass Classifier for P-Glycoprotein Substrates, Inhibitors, and Non-Active Compounds. Molecules 2019; 24: 2006.

22) Lan J, Ge J, Yu J, Shan S, Zhou H, Fan S, Zhang Q, Shi XL, Wang QS, Zhang LQ, Wang XQ. Structure of the SARS-CoV-2 spike receptor-binding domain bound to the ACE2 receptor. Nature 2020; 581: 215-220.

23) Guruprasad L. Human SARS CoV-2 spike protein mutations. Proteins 2021; 89: 569-576.

24) Jangra S, Ye C, Rathnasinghe R, Stadlbauer D; Personalized Virology Initiative study group; Krammer F, Simon V, Martinez-Sobrido L, García-Sastre A, Schotsaert M. SARS-CoV-2 spike E484K mutation reduces antibody neutralisation. Lancet Microbe 2021; 2: e283-e284.

25) Li Q, Nie J, Wu J, Zhang L, Ding R, Wang H, Zhang Y, Li T, Liu S, Zhang MY, Zhao CY, Liu H, Nie LL, Qin Y, Wang M, Lu Q, Li XY, Liu JK, Liang HY, Shi Y, Shen YL, Xie LZ, Zhang LQ, Qu XW, Xu WB, Huang WJ, Wang YC. SARS-CoV-2 501Y.V2 variants lack higher infectivity but do have immune escape. Cell 2021; 184: 2362-2371e9.

26) Thiel V, Ivanov KA, Putics A, Hertzig T, Schelle B, Bayer S, Weißbrich B, Snijder EJ, Rabenau H, Doerr HW, Gorbalenya AE, Ziebuhr J. Mechanisms and enzymes involved in SARS coronavirus genome expression. J Gen Virol 2003; 84: 2305-2315.

27) Narayanan A, Narwal M, Majowicz SA, Varricchio C, Toner SA, Ballatore C, Brancale A, Murakami KS, Jose J. Identification of SARS-CoV-2 inhibitors targeting Mpro and PLpro using in-cell-protease assay [J]. Commun Biol 2022; 5: 169.

28) Baig MH, Sharma T, Ahmad I, Abohashrh M, Alam MM, Dong JJ. Is PF-00835231 a Pan-SARS-CoV-2 Mpro Inhibitor? A Comparative Study [J]. Molecules 2021; 26: 1678.

29) Zhang LC, Zhao HL, Liu J, He L, Yu RL, Kang CM. Design of SARS-CoV-2 Mpro, PLpro dual-target inhibitors based on deep reinforcement learning and virtual screening [J]. Future Med Chem 2022; 14: 393-405.

30) Tong X, Keung W, Arnold LD, Stevens LJ, Pruijssers AJ, Kook S, Lopatin U, Denison M, Kwong AD. Evaluation of in vitro antiviral activity of SARS-CoV-2 M(pro) inhibitor pomotrelvir and cross-resistance to nirmatrelvir resistance substitutions [J]. Antimicrob Agents Chemother 2023; 67: e0084023.

31) Huff S, Kummetha IR, Tiwari SK, Huante MB, Clark AE, Wang S, Bray W, Smith D, Carlin AF, Endsley M, Rana TM. Discovery and Mechanism of SARS-CoV-2 Main Protease Inhibitors [J]. J Med Chem 2022; 65: 2866-2879.

32) Shi Y, Dong L, Ju Z, Li Q, Cui Y, Liu Y, He J, Ding X. Exploring potential SARS-CoV-2 Mpro non-covalent inhibitors through docking, pharmacophore profile matching, molecular dynamic simulation, and MM-GBSA [J]. J Mol Model 2023; 29: 138.

33) Yoshino R, Yasuo N, Sekijima M. Identification of key interactions between SARS-CoV-2 main protease and inhibitor drug candidates [J]. Sci Rep 2020; 10: 12493.

34) Yan W, Zheng Y, Zeng X, He B, Cheng W. Structural biology of SARS-CoV-2: open the door for novel therapies. Signal Transduct Target Ther 2022; 7: 26.

35) Zhu W, Xu M, Chen CZ, Guo H, Shen M, Hu X, Shinn P, Thomas CK, Michael SG, Zheng W. Identification of SARS-CoV-2 3CL Protease Inhibitors by a Quantitative High-Throughput Screening. ACS Pharmacol Transl Sci 2020; 3: 1008-1016.

36) Blanchard JE, Elowe NH, Huitema C, Fortin PD, Cechetto JD, Eltis LD, Brown ED. High-throughput screening identifies inhibitors of the SARS coronavirus main proteinase. Chem Biol 2004; 11: 1445-1453.